(12)

TECHNICAL REPORT NO. 25

TO

THE OFFICE OF NAVAL RESEARCH
CONTRACT No. N00014-76-C-0037, NR 031-756

# THE INFLUENCE OF STRAIN RATE AND POROSITY ON THE DEFORMATION AND FRACTURE OF TITANIUM AND NICKEL

P. E. MAGNUSEN,[+] P. S. FOLLANSBEE,[*] AND D. A. KOSS[+]

[+]DEPARTMENT OF METALLURGICAL ENGINEERING
MICHIGAN TECHNOLOGICAL UNIVERSITY
HOUGHTON, MI 49931

[*]LOS ALAMOS NATIONAL LABORATORY
LOS ALAMOS, NM 87545

SECURITY CLASSIFICATION OF THIS PAGE (When Data Entered)

| REPORT DOCUMENTATION PAGE | | READ INSTRUCTIONS BEFORE COMPLETING FORM |
|---|---|---|
| 1. REPORT NUMBER<br>No. 25 | 2. GOVT ACCESSION NO.<br>AD-A148 670 | 3. RECIPIENT'S CATALOG NUMBER |
| 4. TITLE (and Subtitle)<br>The Influence of Strain Rate and Porosity on the Deformation and Fracture of Titanium and Nickel | | 5. TYPE OF REPORT & PERIOD COVERED<br><br>6. PERFORMING ORG. REPORT NUMBER |
| 7. AUTHOR(s)<br>P. E. Magnusen, P. S. Follansbee, and D. A. Koss | | 8. CONTRACT OR GRANT NUMBER(s)<br>N00014-76-C-0037<br>NR 031-756 |
| 9. PERFORMING ORGANIZATION NAME AND ADDRESS<br>Department of Metallurgical Engineering<br>Michigan Technological University<br>Houghton, MI 49931 | | 10. PROGRAM ELEMENT, PROJECT, TASK AREA & WORK UNIT NUMBERS |
| 11. CONTROLLING OFFICE NAME AND ADDRESS<br>Office of Naval Research<br>800 N. Quincy St.<br>Arlington, VA 22217 | | 12. REPORT DATE<br>July, 1984<br>13. NUMBER OF PAGES |
| 14. MONITORING AGENCY NAME & ADDRESS(if different from Controlling Office) | | 15. SECURITY CLASS. (of this report)<br>Unclassified<br>15a. DECLASSIFICATION/DOWNGRADING SCHEDULE |

16. DISTRIBUTION STATEMENT (of this Report)

Distribution of this document is unlimited

17. DISTRIBUTION STATEMENT (of the abstract entered in Block 20, if different from Report)

18. SUPPLEMENTARY NOTES

19. KEY WORDS (Continue on reverse side if necessary and identify by block number)

Strain Rate, Porosity, Deformation, Fracture, Titanium, Nickel

20. ABSTRACT (Continue on reverse side if necessary and identify by block number)
The influence of strain rate on the tensile deformation and fracture behavior of powder-fabricated titanium and nickel containing porosity has been investigated. Measurements of uniform strain, local fracture strains, and elongations to failure show that, over the range of strain rates from $10^{-4}$ to $10^{2}s^{-1}$, there is little or no effect of the strain rate on the fracture behavior of these materials at any of the porosity levels studied. In contrast, increasing porosity causes significant decreases in the yield stress, strain-hardening exponent, and ductility; these effects are more pronounced in the titanium than in the nickel.

DD FORM 1 JAN 73 1473 EDITION OF 1 NOV 65 IS OBSOLETE
S/N 0102-LF-014-6601

SECURITY CLASSIFICATION OF THIS PAGE (When Data Entered)

20. Abstract - Continued

The porosity-induced loss of ductility can be understood in terms of the combined effect of enhanced geometric softening and shear localization due to a network of imperfections introduced into the materials by the presence of porosity. Secondary effects due to hydrogen embrittlement and thermal gradients forming during deformation are also noted.

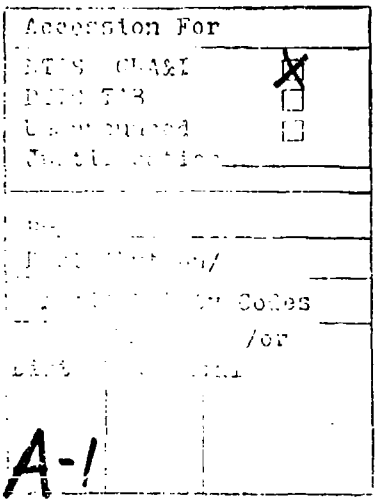


# The Influence of Strain Rate and Porosity on the Deformation and Fracture of Titanium and Nickel

P. E. Magnusen,* P. S. Follansbee,+ and D. A. Koss*

*Department of Metallurgical Engineering
Michigan Technological University
Houghton, Michigan 49931

+Los Alamos National Laboratory
Los Alamos, New Mexico 87545

## ABSTRACT

The influence of strain rate on the tensile deformation and fracture behavior of powder-fabricated titanium and nickel containing porosity has been investigated. Measurements of uniform strain, local fracture strains, and elongations to failure show that, over the range of strain rates from $10^{-4}$ to $10^{2}$ $s^{-1}$, there is little or no effect of the strain rate on the fracture behavior of these materials at any of the porosity levels studied. In contrast, increasing porosity causes significant decreases in the yield stress, strain-hardening exponent, and ductility; these effects are more pronounced in the titanium than in the nickel. The porosity-induced loss of ductility can be understood in terms of the combined effects of enhanced geometric softening and shear localization due to a network of imperfections introduced into the materials by the presence of porosity. Secondary effects due to hydrogen embrittlement and thermal gradients forming during deformation are also noted.

## INTRODUCTION

The influence of strain rate on the room temperature yield and flow stress of metals in well documented.[1] It is also well known that the presence of porosity decreases the yield stress and reduces the tensile ductility of metals [see, for example, refs. 2-4]. However, the influence of strain rate on the room temperature deformation and fracture of metals containing porosity has not been studied in detail. Given a ductile fracture process in which failure occurs by void nucleation, growth, and link-up, it is likely that the failure of porous metals under high temperature creep conditions will be sensitive to strain rate. However, pre-existing porosity usually does not limit the utilization of alloys by its effect on creep behavior; a more typical limitation is the accompanying loss of tensile ductility and high cycle fatigue resistance at low temperatures. Thus the purpose of this study is to examine the influence of strain rate, over a range $10^{-4}$ to $10^{2}s^{-1}$, on the room temperature tensile deformation and fracture of powder-fabricated Ti and Ni containing various levels of rounded porosity, from near fully dense to 9% porosity. The Ti and Ni have been chosen because of their contrasting strain and strain-rate hardening behavior. At room temperature, the flow stress of commercially pure (CP) Ti is considerably more sensitive to strain rate[5,6] and temperature[6,7] than is Ni[8] while fully dense Ni exhibits a much higher strain hardening rate[8] than does Ti.[9] Finally, it should be noted that, although this study pertains to metals containing porosity, there is a marked lack of fracture data on fully dense alloys in the $10^{-1}$ to $10^{2}s^{-1}$ range; the present results also contain implications for such cases.

## EXPERIMENTAL PROCEDURE

The materials used in this study were powder-fabricated to various levels of porosity using cold isostatic pressing, swaging, and sintering processes. The Ti powder was produced from electrolytic sponge by a hydride-dehydride process at Teledyne-Wah Chang. Most (57%) of the Ti powder was in the -70 to +140 mesh range, and it contained 1290 wt. ppm oxygen and only 50 wt. ppm chlorine. The as-supplied, atomized Ni powder was sieved to provide a better particle size match to the Ti powder; 63% of the resulting nickel powder was in the -140 to +325 mesh range, and it contained considerable sulfur: 150 wt. ppm.

To control porosity levels, the Ti was cold isostatically pressed, vacuum sintered at 1400°C; for the two highest density levels, it was subsequently swaged various levels, and re-sintered at 1400°C.[10] The resulting microstructures, as shown in Fig. 1, consist of rounded porosity at levels of 0.1%, 1.5%, 4.0%, and 6.7% porous.* In all cases, the largest fraction of pores were in the 7-14 μm diameter range while the grain sizes were in the 100-140 μm range.

Considerable care was required to prepare the Ni specimens containing the desired levels of rounded porosity and a fine grain size. This was accomplished by cold isostatically pressing at 380 MPa and sintering at 1150°C for 12 hrs., which yielded material containing 9.4% porosity. For higher density material, the sintered compact was subsequently swaged either 15% or 70% reduction in area, and re-sintering at 1100°C or 900°C respectively; these resulted in porosity levels of 4.1 and 0.5%, respectively. To minimize a sulfur-induced temper embrittlement problem at the higher densities, a rapid air cool from the re-sintering temperature was used. The resulting

*The densities of both the Ti and Ni specimens were obtained by an immersion technique (ASTM Standard B328) and confirmed by quantitative metallography.

microstructures are shown in Fig. 2. The pore sizes in the Ni (<7 μm pore diameter) are somewhat smaller than those in the Ti, and the Ni grain sizes were also smaller, ranging from 30-60 μm.

Tensile specimens consisted of round, axisymmetric tensile bars with a 2.25 mm diameter and 17.8 mm gauge length. Tests at strain rates of 1 to $10^2 s^{-1}$ were performed in a servo-hydraulic test machine with specially designed grips to allow a short acceleration distance at the start of the test (see ref. 10 for a more detailed description of the apparatus and procedure). Tests at $1.2 \times 10^{-4}$ and to $1.2 \times 10^{-2} s^{-1}$ were conducted in an electro-mechanical testing machine using the same specimen grips as above but coupled to the low strain-rate machine by an adapter. In all cases testing was performed at room temperature.

## EXPERIMENTAL RESULTS

### A. The Influence of Strain Rate

The influence of strain rate on the flow stress of near fully dense Ti and Ni at true strains of $\varepsilon=0.02$ and $\varepsilon=0.2$ is shown in Fig. 3. As shown, the strain-rate hardening exponent $m=d\ln\sigma/d\ln\dot{\varepsilon}$ increases slightly with strain for both Ti and Ni. For Ti, the value of $m=0.021$ at $\varepsilon=0.2$ is identical to that observed previously also at $\varepsilon=0.2$ for fully dense material.[9] The strain-rate hardening exponents for the 1.5, 4.0, and 6.7% porous Ti specimens have also been determined near maximum load; these are 0.020, 0.023, and 0.025, respectively. In contrast to the Ti, the m-values for the Ni are much smaller (approximately half) and increase slightly at strain rate at $\dot{\varepsilon}>10 s^{-1}$. At the lower $\dot{\varepsilon}$ range, the value of m for the 0.5% porous Ni ($m=0.009$ at $\varepsilon=0.2$) compares favorably with $m=0.010$ for the 4.1 and 9.4% porous Ni specimens at $\varepsilon=0.1$. Given the values of m for both Ti and Ni over a range of porosity

levels, we conclude that the strain-rate hardening exponent is essentially independent of pore content for both Ti and Ni.

The value of the strain hardening exponent $n=d\ln\sigma/d\ln\dot{\varepsilon}$ has also been determined for both Ti and Ni over the entire range of strain rates. There is no systematic influence of strain rate on n for $10^{-4} \leq \dot{\varepsilon} \leq 10^{2} s^{-1}$.

The local (true) fracture strain $(\varepsilon_f)^*_{local}$, the elongation to failure over the entire gauge length $e_f$, and the (true) strain at maximum load $\varepsilon_{max\ load}$ have been determined, and Figs. 4 and 5 show that, for both Ti and Ni, all are nearly insensitive to strain rate over the range of strain rates from $10^{-4}$ to $10^{2} s^{-1}$. In the case of the Ti, the elongation to failure shows a weak minimum at $\dot{\varepsilon} \sim 1 s^{-1}$ in the 0.1 and 1.5% porous specimens, while the 0.5% porous Ni exhibits an increase in both $(\varepsilon_f)_{local}$ and $e_f$ at $\dot{\varepsilon} > 10 s^{-1}$. The strain at maximum load is commonly used as a criterion for the onset of diffuse necking and, according to the Considere criterion, should equal the strain hardening exponent n. As shown in Figs. 4 and 5, $\varepsilon_{max\ load} \simeq n$ for both Ti and Ni in the near fully dense conditions. This relationship is well obeyed for all porosity levels in the Ti, but the uniform strains in the 4.1 and 9.4% porous Ni are lower than the corresponding n-values.

Figures 6 and 7 show representative scanning electron micrographs of the fracture surfaces of the Ti and Ni tested at the extremes of the strain-rate range and pore contents. Strain rate has no apparent effect on the appearance of the fracture surface in the Ti at any of the pore contents; see Fig. 6. In all cases, failure occurs in the Ti by a ductile fracture process characterized by a dimpled fracture appearance. Longitudinal sections also show no apparent difference in the degree of tortuosity of the fracture path among the strain rate.

---

*This is the value of the maximum principal strain across the fracture surface based on two orthogonal thickness strain measurements and an assumption of conservation of volume.

In the case of the Ni, strain rate has a definite effect on the fracture surface appearance at the 0.5% porosity level but not in the 9.4% material (or the 4.1% porous Ni). As shown in Fig. 7, the 0.5% porous specimens exhibit a dimpled, transgranular fracture surface at $\dot{\varepsilon}=10^{2}s^{-1}$ (and at $10s^{-1}$) as do the 9.4 and 4.1% porous specimens at all strain rates (check this). However, with decreasing strain rate the fracture mode progressively changes so that at $\dot{\varepsilon}=10^{-4}s^{-1}$, the fracture surface shows extensive intergranular failure.

The increase in the volume fraction of pores with strain has also been determined for the Ni containing 9.4% porosity at strain rates of $10^{-4}s^{-1}$ and $10^{2}s^{-1}$. These data show that, within experimental error, there is no influence of strain rate on the pore/void growth rate.

B. The Influence of Porosity

Increasing the volume fraction of porosity decreases the yield stress (Fig. 8), the strain-hardening exponent $n=d\ln\sigma/d\ln\varepsilon$ (Fig. 9) and the elongation to failure (Fig. 10) of Ti as well as Ni. The effects are more pronounced in the Ti than in the Ni. The decrease in yield stress with increasing porosity is a well established effect in sintered P/M alloys.[2] In the present study, a yield strength decrease occurs at all strain rates, but in Ti it is significant only above the 1.5% porosity level; see Fig. 8.

The decrease in strain hardening exponent n with increasing porosity, as shown in Fig. 9, has been occasionally observed in porous materials.[3,11] In the present case, the values of n have been determined for $0.02\leq\varepsilon\leq\varepsilon_{\text{max load}}$, with the exception of the 0.1% porous Ti which exhibits $n=f(\varepsilon)$ for $\varepsilon<0.1$; in this case the n-value is based on the strain range $0.1\leq\varepsilon\leq\varepsilon_{\text{max load}}$. For both Ti and Ni, the n-values are independent of strain rate although they do show the scatter indicated in Fig. 9. It might be noted that, as expected, the n-values of Ni exceed those of Ti by a factor of 2-3. This is consistent

with the values of n for fully dense, wrought Ti (n=0.16-17[9]) and Ni (n=.5-.6[8]).

As previously noted, the strain-rate hardening exponent m is not affected by porosity level. For Ti, m~0.022 and for Ni m~0.010 at all levels of porosity.

The elongation to failure $e_f$ decreases with increasing porosity in the manner shown in Fig. 10. This figure includes data at all strain rates except for Ni at $10^2 s^{-1}$, which shows an increase in $e_f$ with increasing $\dot{\varepsilon}$ (see Fig. 5). The data form two well-defined trend lines, with the rate of ductility loss being greater in the Ti than in the Ni. If the 4.1% porous Ni ductilities were included, they would appear anomolously low (see Fig. 5). However, as shown in Fig. 7 quantitative fractography indicates that the projected area fraction of pores on the fracture surface of the 4.1% porous Ni is at least as great as in the Ni containing 9.4% porosity. Thus pore content of the eventual fracture plane of these two materials is nearly the same even though the bulk pore level differs by a factor of two; the consequences of this will be discussed later.

As observed previously[12] and suggested above, a common feature of the fracture surface of porous metals, as may be noted in Figs. 6 and 7, is that the area fraction of pores on the fracture surface is much greater than the bulk pore content. In the present study, an unambiguous determination of the projected area fraction of pores is difficult, but rough estimates indicate the pore area fraction is roughly 7 times the initial bulk pore fraction for the Ti and ranges from a factor of at least 4 for the 9.4% porous Ni to about 10 for the Ni containing 4.1% porosity.

## DISCUSSION

Over the strain-rate range of $10^{-4}$ to $10^2 s^{-1}$, the strain rate increases the flow stress (Fig. 3) but it does not affect the fracture behavior at any

level of porosity in either Ti or Ni (Figs. 4 and 5). The nearly constant strain-rate sensitivity of the flow stress of Ti and Ni is consistent with previous investigators who observe no increase in m with strain rate until $\dot{\varepsilon}>4\times10^{2}s^{-1}$ for Ti[3] and $\dot{\varepsilon}>5\times10^{2}s^{-1}$ for Ni.[8] In the present study, the Ni data show m to increase with strain rate for $\dot{\varepsilon}>10s^{-1}$. An increase in the rate sensitivity of Ni at high strain rates has been measured previously,[8] and it has been suggested that this is due to a change in deformation mechanism.[13]

The most significant result of this study regarding strain-rate effects is the absence of any pronounced effect of strain rate on the fracture behavior of either Ti or Ni containing porosity. Two minor effects are evident: (1) a modest ductility minimum in the elongation-to-failure data of Ti (Fig. 2b), and (2) an increase in local fracture strain and elongation-to-failure in the near-fully dense Ni (Figs. 5a and 5b) at high strain rates. In the latter case, the ductility increase is most likely associated with the increased strain-rate sensitivity of Ni at high strain rates (which would increase post-uniform extension[14]) and with a suppression of intergranular fracture probably caused by hydrogen sweep-in at low strain rates[15] (see note*). The ductility minimum in Ti may be understood if it is recognized that since the $\varepsilon_{\text{max load}}$ data are not affected by strain rate (see Fig. 2b), any influence of strain rate on total elongation to failure must be due to changes in post-uniform elongation behavior. Thermal gradients along the length of the specimen will become most pronounced during diffuse necking and, for a material with a temperature-dependent flow stress such as Ti, induce flow softening.[13,16] This effect should be most pronounced at intermediate strain

*In the Ni containing isolated porosity, a possible source of hydrogen is the sintering atmosphere which becomes trapped within the Ni as the sintering isolates the pores (which does not occur at 9.1% porosity) and the material is cooled rapidly.

rates because of the competition between heat generation due to plastic deformation, which will be greatest during diffuse necking, and heat flow along the specimen into the grips. When a diffuse neck occurs near the center of the gauge length, the heat flow effect will accentuate the thermal gradient and flow softening will further localize deformation, reducing ductility.[17] The effect will also be most pronounced in a material such as near-fully dense Ti which shows considerable post-uniform extension; compare $\varepsilon_{\text{max load}}$ to $(\varepsilon_f)_{\text{local}}$ data in Fig. 4. At higher porosity levels, there is not sufficient post-uniform strain to trigger this thermal effect.

The absence of any strong influence of strain rate on the fracture behavior of Ti and Ni over a range of pore contents may be understood in the context of ductile fracture of porous metals. First, these results are consistent with the expectation that at relatively low temperatures, such as room temperature, there appears to be very little, if any, rate sensitivity to void formation, void growth [as observed in the Ni-9.4% porous material], or void link-up. This lack of rate sensitivity may also be inferred from the comparatively small changes of flow stress with strain rate ($m < 0.02$) and from the insensitivity of the strain-hardening and strain-rate hardening behavior to strain rate (Figs. 3 and 9). Assuming the ductile fracture process to be controlled by the stress-strain response of a given material, it is not surprising that strain rate has little or no influence on the fracture strains of the near-fully dense Ti and Ni. In addition to the above, the relative insensitivity of fracture in the porous materials also reflects the rate insensitivity of the shear instability which appears to control void link-up in porous materials.[12] In such a concept, the presence of pores introduces into the material a network of planes of high pore content ("imperfections") which eventually cause shear localization and limit the ductility of the material.[12] While ductility in such a case is sensitive to

strain-rate hardening, it should not be influenced by absolute strain rate so long as m≠f(ε̇). Except for Ni at the highest strain rate, this is the case in the present study.

The influence of porosity on ductility has been shown to be relatively strong in these experiments. There are at least two mechanisms that contribute to a loss of ductility with increasing porosity: (1) a decrease in uniform elongation and (2) porosity-triggered shear instabilities. In the first mechanism, geometrical softening will decrease uniform elongation with increasing porosity due to the combination of a decreased n-value and strain-induced pore growth.* There are two approaches to analyzing geometric softening and uniform elongation in porous metals. In one approach,[18,19] the intrinsic stress σ - strain ε behavior of the matrix is assumed to obey a $\sigma = K\varepsilon^{n'}$ relationship, and the effect of porosity on uniform strain $\varepsilon_u$ is calculated on the basis of the initial volume fraction of porosity $f_o$ and the volume fraction of porosity f at a strain ε. Two expressions have been obtained on this basis.[18,19] Taking into account void growth and using a load instability criterion for diffuse necking, Dodd and Atkins obtain[18]

$$\varepsilon_u = \frac{n'(1-f)}{df/d\varepsilon} \quad . \tag{1}$$

Since $(f/f_o) = 1 + 1.5\varepsilon$ for CP Ti with porosity,[10] Eq. 1 badly underpredicts the magnitude of the decrease in ductility with increasing porosity. A second analysis by Stevenson,[19] also is based on a load instability and accounts for strain-induced void growth but results in the following expression for the uniform strain.

*It should be noted that the decrease in n-value is much greater than that predicted by the loss of load carrying capacity due to strain-induced pore growth.

$$\varepsilon_u = \frac{n' - f_o}{1 + f_o} \qquad (2)$$

Equation 2 predicts a relationship between the work hardening exponent of the porous material n and that of the matrix n' which is $n = n' - f_o (1 + n')$. Such a relationship describes the Ti data in Fig. 9 very well but is in poor agreement with the n-values of porous Ni in Fig. 9. In addition, Eq. 2 also is not accurate in predicting the observed decrease in uniform strain with porosity at small (<5%) pore contents.

An alternate approach is to assume that the work hardening exponent n of the porous material is known as a function of initial pore content (for example, Fig. 9) and that the uniform strain for the onset of diffuse necking is basically $\varepsilon_u$ = n+(correction term for strain-induced pore growth). Such an analysis (see Appendix I) yields:

$$\varepsilon_u \simeq \frac{n(1-f_o)}{[1-f_o-af_o]} \qquad (3)$$

for a material with an initial volume fraction $f_o$ of porosity which undergoes strain-induced pore growth according to a $f/f_o = 1$ rac relationship.[17] Figure 11 indicates reasonably good agreement, especially for the Ti, between the predictions of Eq. 3 and the observed dependences of uniform strain on initial pore content. This analysis, which is based on the experimental values of n, indicates that porosity should clearly cause a decrease in tensile ductility due to a decrease in uniform strain at the onset of diffuse necking.

Figures 4 and 5 show that the relative decreases in the total elongation and the maximum local fracture strain exceed that in the strain at maximum load. This result, which is especially evident for the case of Ti, suggests that during diffuse necking another mechanism must contribute to the loss of

ductility with increasing porosity. One possible mechanism would be thermoplastic instability, as modelled by Dodd and Atkins.[18] However, this process should show a dependence on strain rate; since strain rate has been shown to have little effect on ductility in these studies, it seems unlikely that thermoplastic instability is a major mechanism of strain localization in these experiments. A more probable explanation for the decrease in ductility during diffuse necking is that the presence of porosity introduces planes of high pore content or imperfections into the material on a local scale. As the volume fraction of porosity increases, the level of porosity on such planes, or the size of the imperfection, increases. In both instances, this results in a rapid decrease in ductility which is more severe in the low work-hardening Ti than in the Ni (Fig. 10). A characteristic of such a process is the high level of porosity evident on the fracture surfaces (Figs. 6 and 7).

Finally, we note that the "anamolously" low ductility of the 4.1% porous Ni can also be readily understood in terms of the imperfection concept. It may be recalled that the fracture surface of this material contains at least the same pore content as that of the 9.4% porous Ni. Thus a non-uniform pore distribution causes a large imperfection in the 4.1% porous material which actually exceeds that of the 9.4% porous material. As a result, the tensile ductility in the Ni w/4% porosity is actually less than that of the Ni w/9% porosity (Fig. 5). It should also be noted that the 4.1% porous Ni also shows a 22% lower yield stress than the 0.5% porous Ni; this is also consistent with the presence of a large imperfection.[9]

## SUMMARY

The influence of strain rate on the tensile deformation and fracture of powder-fabricated titanium and nickel containing levels of porosity from 9% to near-fully dense may be summarized as follows:

1) Over a range $10^{-4}$ to $10^{2}s^{-1}$, the strain rate has only minor effects on either the uniform strain, local fracture strain, or tensile elongation to failure. The absence of any strong effect on fracture may be understood in terms of the lack of any strong rate sensitivity of void formation, growth, and link-up at room temperature and in terms of the failure of porous materials being controlled by shear instabilities developing along planes of high pore content.

2) Two minor ductility effects are observed. The first, a weak minimum in elongation to failure in Ti containing 0.1 and 1.5% porosity, appears to be caused by thermal gradients developing due to diffuse necking and incomplete heat dissipation along the specimen length. The second, a small ductility increase at high strain rates in Ni, appears to be caused by a combination of increased strain-rate sensitivity and decreased susceptibility to hydrogen embrittlement at high strain rates.

3) As observed previously in fully dense Ti and Ni,[3,4] the flow stresses of both Ti and Ni increase with increasing strain rate such that $m=d\ln\sigma/d\ln\dot{\varepsilon}\simeq 0.022$ for Ti and $\simeq 0.010$ for Ni. Within the experimental error, the m-values are independent of porosity level.

The influence of porosity on the tensile deformation and fracture of Ni and Ti over the strain rate range examined has the following effects:

(1) Increasing porosity causes concomitant decreases in the (a) yield stresses (which exceed those predicted by the rule of mixtures), (b) ductility, and (c) strain-hardening exponent. In all three cases, the property decreases are greater in the Ti than in the Ni.

(2) At all porosity levels, the fracture surface is characterized by a much higher pore content than is present on a random plane in the bulk, even if strain-induced pore growth is taken into account.

The above effects are qualitatively consistent with the concept that the role of porosity is to enhance geometric softening due to decreasing n-value and strain-induced pore growth as well as creating a network of planes of high pore content which act as imperfections to localize flow.[12]

## ACKNOWLEDGEMENTS

The technical assistance and suggestions of M. G. Stout, R. M. Aikin, and M. Lopez are gratefully acknowledged. This research was jointly supported by the Office of Naval Research through Contract No. N00014-76-C-0037, NR031-76 and by the Department of Energy.

## APPENDIX

Diffuse necking in a strain-rate insensitive material containing an initial volume fraction $f_o$ of porosity and subjected to uniaxial tension can be understood on the following basis. We assume that the stress $\sigma$-strain $\varepsilon$ behavior of the porous material is known and obeys a $\sigma=k\varepsilon^n$ relationship, where k and n are constants. Associating the onset of diffuse necking with maximum load, we require dP=0 in which case

$$\frac{d\sigma}{\sigma} = -\frac{dA_o}{A_o}, \tag{A1}$$

where $A_o$ is the cross section area of the specimen. If f is the volume fraction of porosity, then $A_o(1-f)$ is the cross section area of material comprising the matrix. Since the volume of the matrix remains constant during deformation [we neglect the small amount of void formation which may occur prior to diffuse necking],

$$dV = d[A_o(1-f)l] = 0 \tag{A2}$$

where l is the specimen length. While the extension of the specimen is a result of strain in the matrix, strain-induced pore growth also contributes. The relationship between volume fraction of pores (f) at a given strain and that ($f_o$) initially may be inferred from strain-induced void growth[20] so that

$$f/f_o = 1 + a\varepsilon \tag{A3}$$

where a is a constant sensitive to stress state.[20] For Ti containing 4.5% porosity and deformed in uniaxial tension at room temperature, $a \simeq 1.5$.[12] Combining Eqs. (A1) - (A3) and simplifying by assuming $f_o < 0.1$ and $\varepsilon_u \leq 0.3$, the uniform strain $\varepsilon_u$ is

$$\varepsilon_u \simeq \frac{n(1-f_o)}{(1-f_o-af_o)} \tag{A4}$$

## REFERENCES


1. J. D. Campbell: Mat'l Sci. and Eng., 1973, vol. 12, p. 3.

2. M. Eudier: Powder Metall., 1962, vol. 6, p. 278

3. B. I. Edelson and W. M. Baldwin, Trans. ASM, 1962, vol. 55, p. 230.

4. R. Haynes: Powder Metall., 1977, vol. 20, p. 17.

5. N. Lawson and T. Nichols: J. Mech. Phys. Solids, 1972, vol. 20, p. 65.

6. J. Harding: Arch. Mech. (Poland), 1975, vol. 27, p. 715.

7. H. Conrad: Progress in Materials Science, J. W. Christian, P. Haasen, and T. B. Massalski, eds., Pergamon Press, New York, 1982, p. 123.

8. T. Muller: J. Mech. Eng. Sci., 1972, vol. 14, p. 161.

9. C. W. Lentz, D. A. Koss, M. G. Stout, and S. S. Hecker: Metal. Trans. A, 1983, vol. 14A, p. 2527.

10. P. E. Magnusen, M.S. Thesis, Michigan Technological University, 1984.

11. S. D. El Wakil, in Proc. 12th North American Manuf. Research Conf., Houghton, MI, 1984.

12. R. J. Bourcier, R. E. Smelser, O. Richmond and D. A. Koss, unpublished research.

13. T. Muller: Acta Met., 1971, vol. 19, p. 691.

14. A. K. Ghosh: Acta Met., 1977, vol. 25, p. 1413.

15. J. K. Tien, A. W. Thompson, I. M. Bernstein, and R. J. Richards: Metall. Trans. A, 1967, vol. 7A, p. 821.

16. M. Wada and T. Nakamura: Phil Mag., 1978, vol. 38, p. 167.

17. P. S. Follansbee, unpublished research, Los Alamos National Laboratory.

18. B. Dodd and A. G. Atkins: Acta Met., 1983, vol. 31, p. 9.

19. R. Stevenson: Private Communication, 1984; see also R. Stevenson and A. K. Ghosh, General Motors Research Publication GMR-3999, General Motors Research Laboratories, Warren, MI., Feb. 25, 1982.

20. J. R. Rice and D. M. Tracey: J. Mech. Phys. Solids, 1969, vol. 17, p. 201.

LIST OF FIGURES

Figure 10. The influence of porosity on elongation to failure for Ti and Ni tested over the strain-rate range $10^{-4}s^{-1} \leq \dot{\varepsilon} \leq 10^{2}s^{-1}$.

Figure 11. The dependence of uniform strain on initial porosity content for Ti and Ni as determined experimentally and as predicted from Eq. 3.

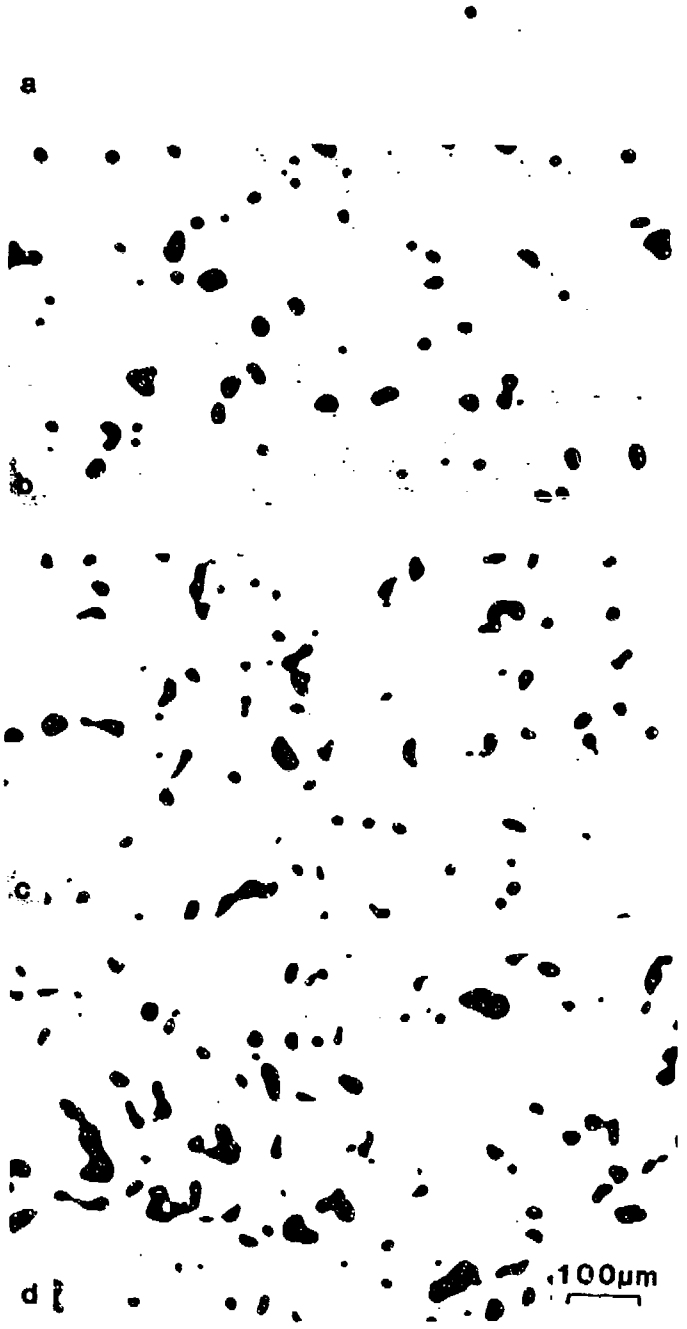


Figure 1. Optical micrographs of porous C.P. titanium containing (a) 0.1% porosity; (b) 1.5% porosity; (c) 4.0% porosity; and (d) 6.7% porosity.

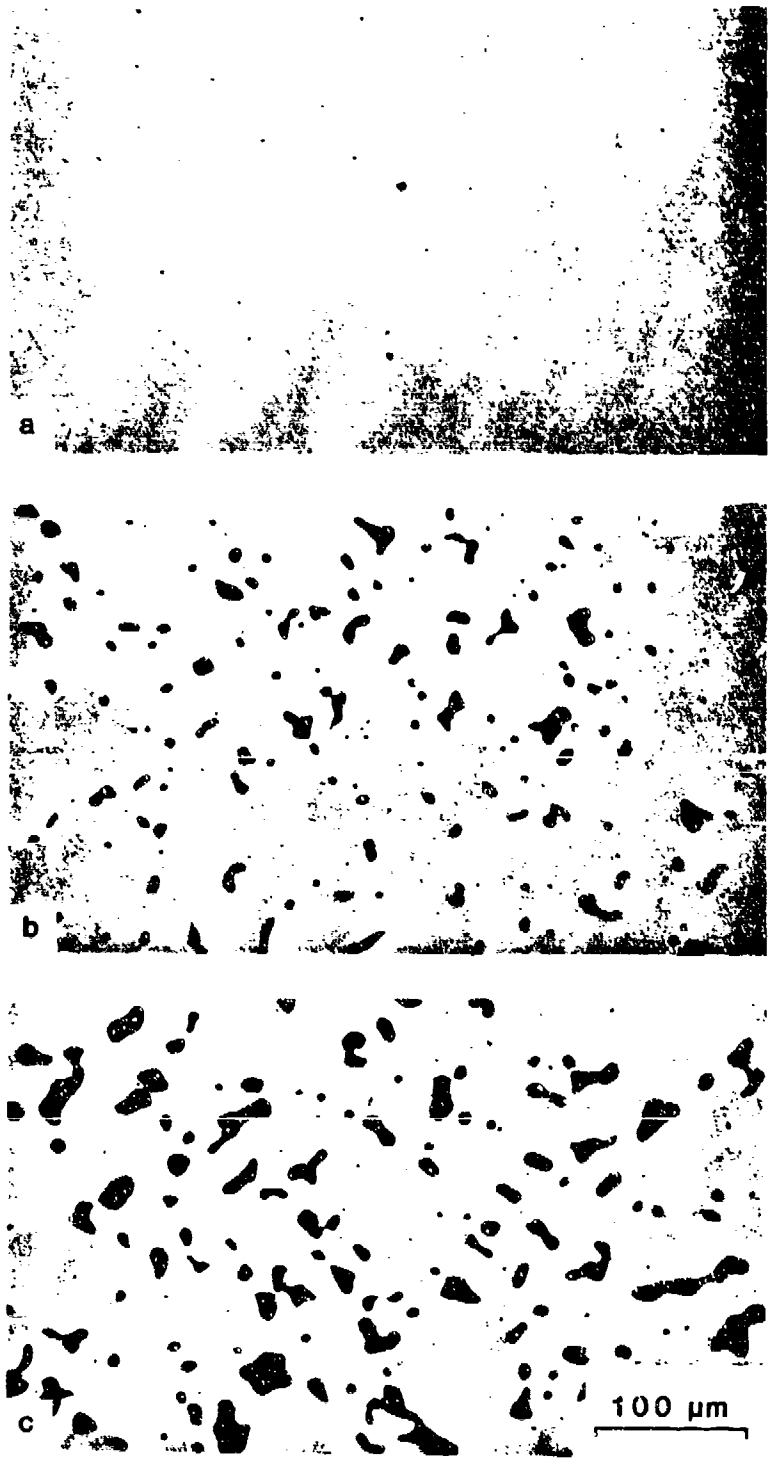


Figure 2. Optical micrographs of porous nickel containing (a) 0.5% porosity; (b) 4.1% porosity and (c) 9.4% porosity.

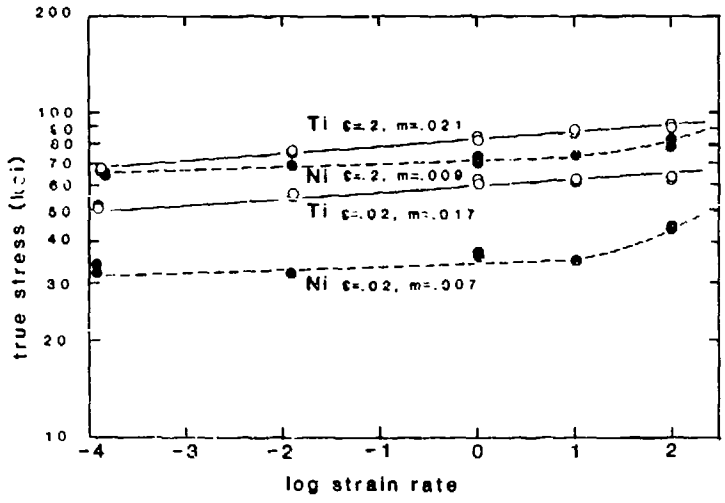


Figure 3. The dependence of flow stress on strain rate for Ti containing 0.1% porosity and Ni containing 0.5% porosity.

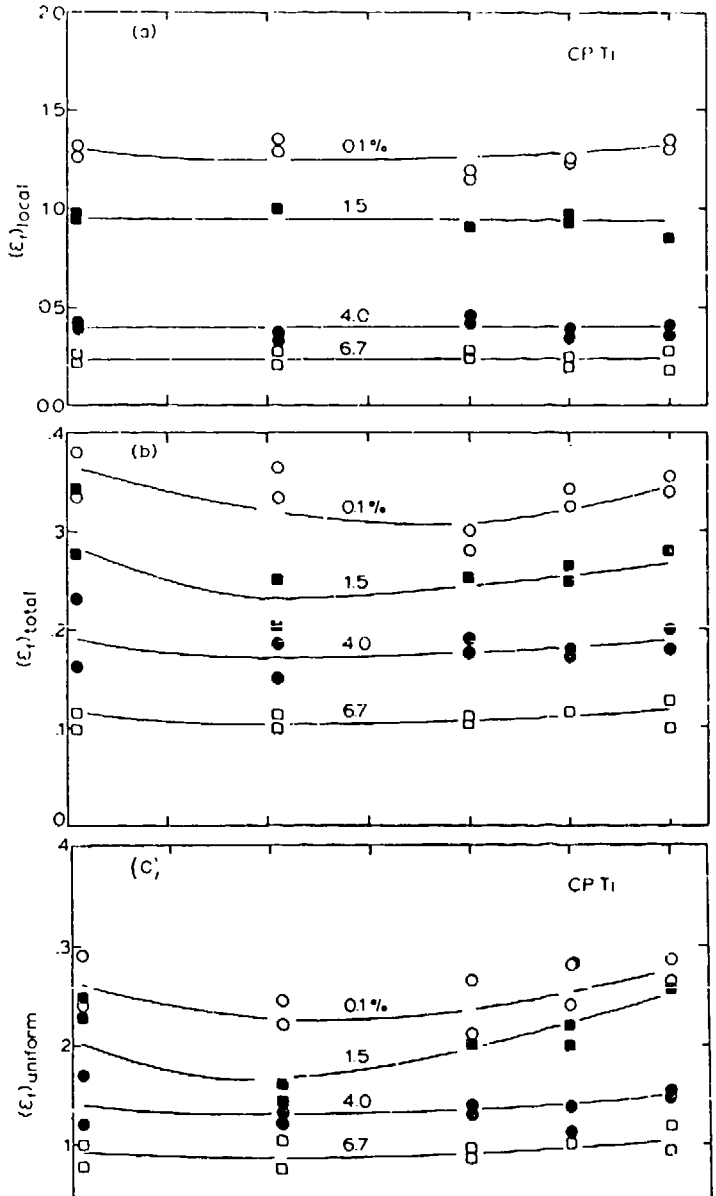


Figure 4. The effect of strain rate on (a) local fracture strain $(\varepsilon_f)_{local}$, (b) elongation to failure $(e_f)$ and (c) true strain at maximum load $(\varepsilon_{max\ load})$ for porous Ti.

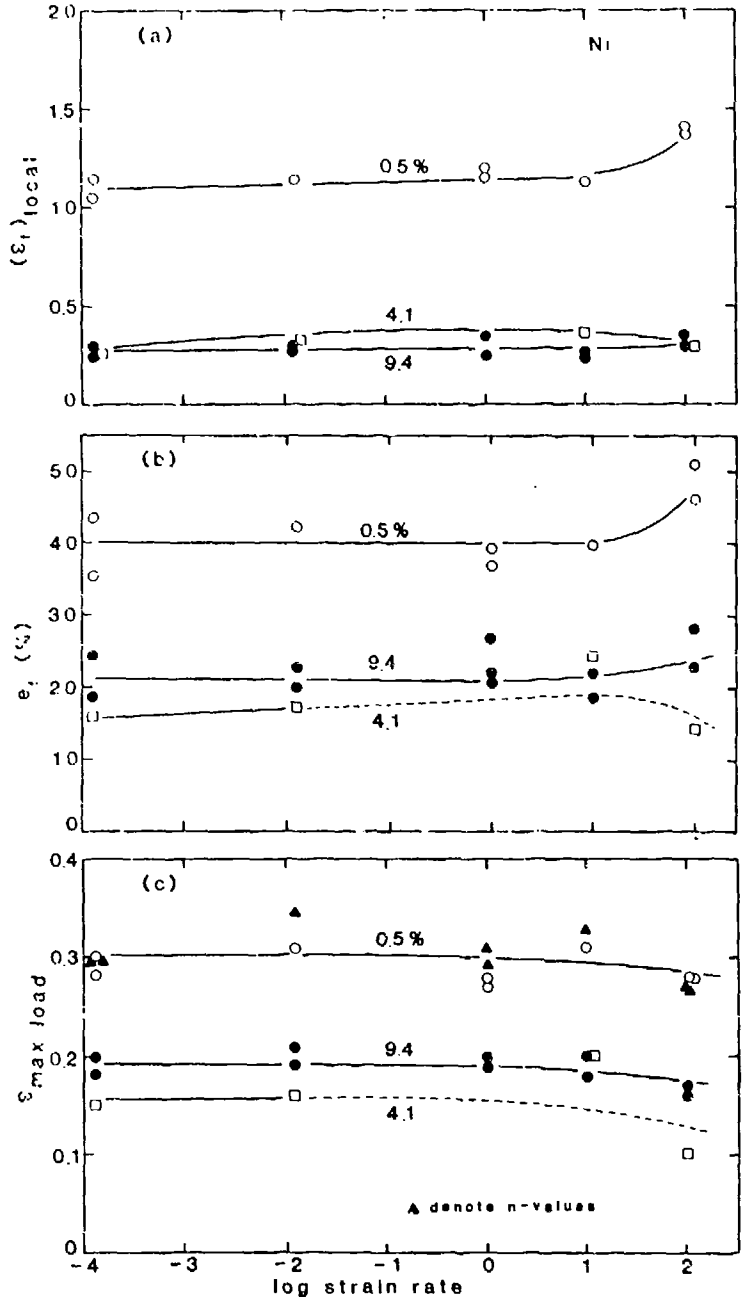


Figure 5. The effect of strain rate on (a) local fracture strain, (b) elongation to failure, and (c) true strain at maximum load for porous Ni.

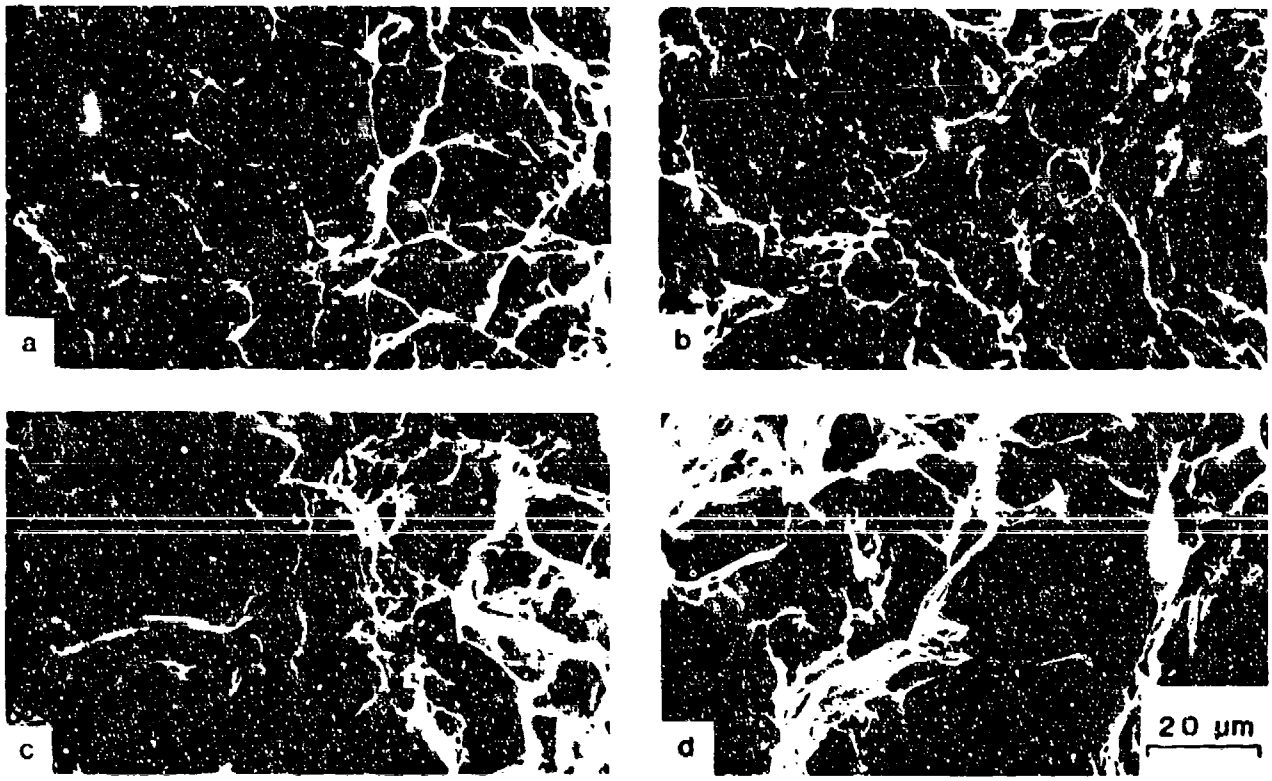


Figure 6. Scanning electron micrographs of the fracture surfaces of Ti at (a) 0.1% porosity and $10^{2}s^{-1}$ strain rate, (b) 0.1% porosity and $10^{-4}s^{-1}$. (c) 6.7% porosity and $10^{2}s^{-1}$, and (d) 6.7% porosity and $10^{-4}s^{-1}$.

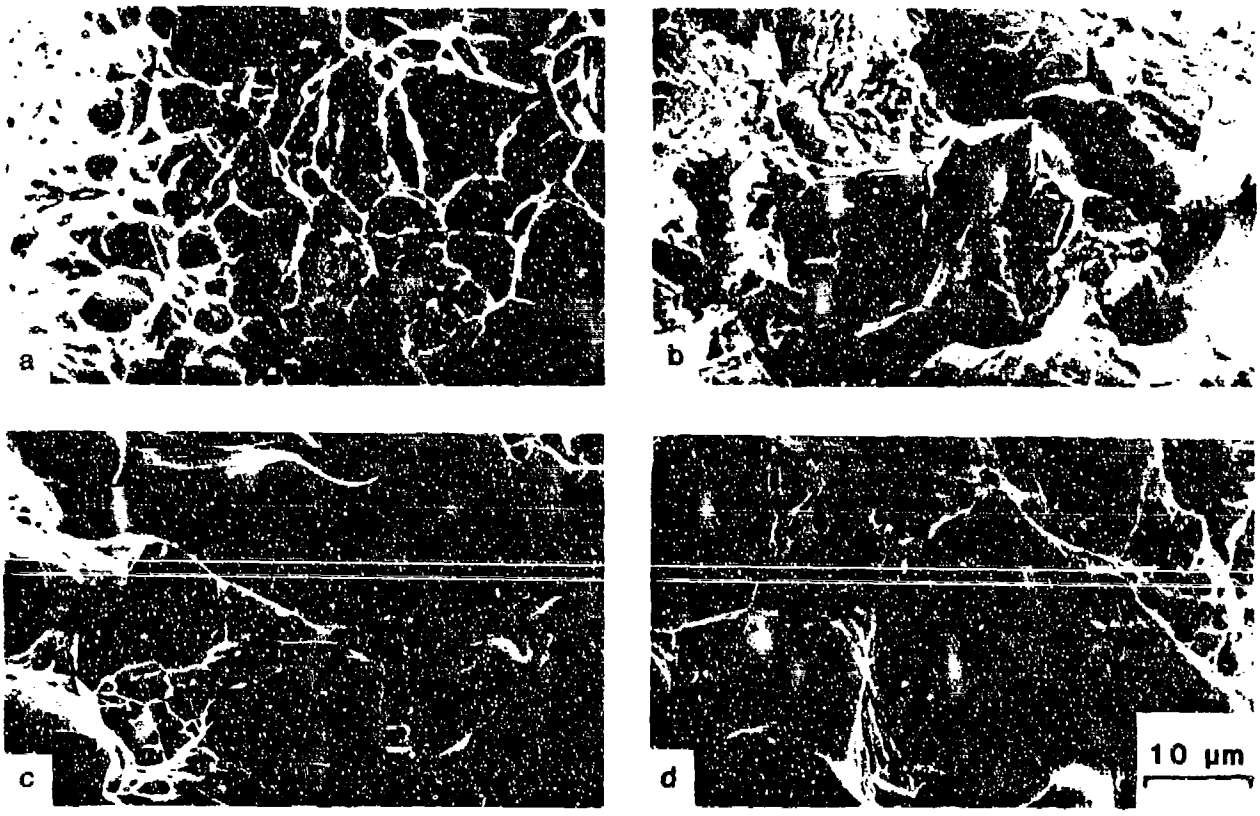


Figure 7. Scanning electron micrographs of the fracture surfaces of Ni at (a) 0.5% porosity and $10^{2}s^{-1}$ strain rate, (b) 0.5% porosity and $10^{-4}s^{-1}$, (c) 9.4% porosity and $10^{2}s^{-1}$, and (d) 9.4% porosity and $10^{-4}s^{-1}$.

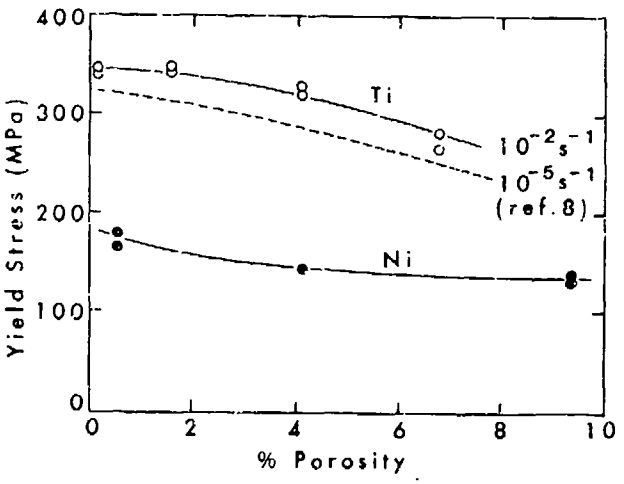


Figure 8. The dependence of yield stress on porosity for Ti and Ni.

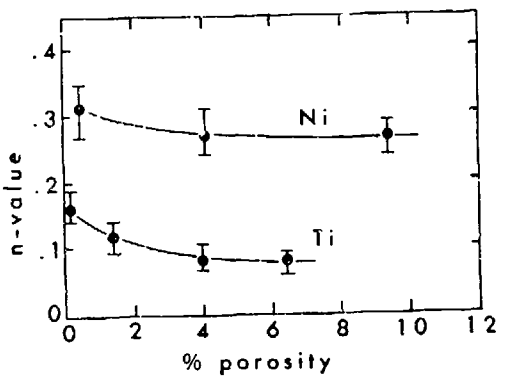


Figure 9. The dependence of the strain hardening exponent n on porosity for Ti and Ni tested over the strain-rate range $10^{-4}s^{-1} \leq \dot{\varepsilon} \leq 10^{2}s^{-1}$.

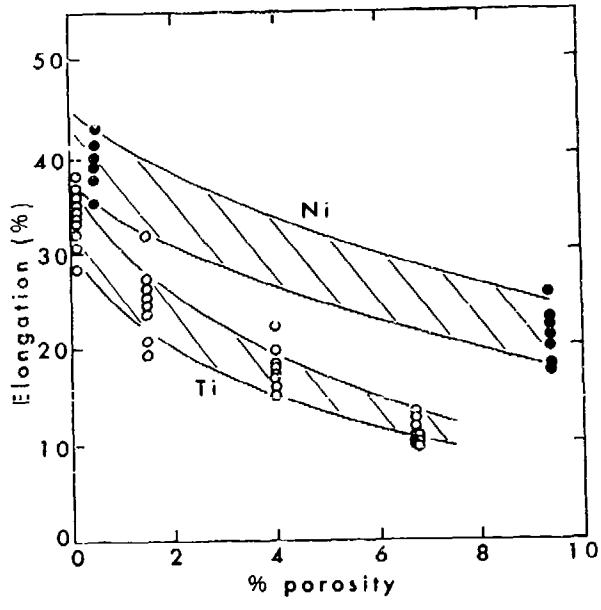


Figure 10. The influence of porosity on elongation to failure for Ti and Ni tested over the strain-rate range $10^{-4}s^{-1} \leq \dot{\varepsilon} \leq 10^{2}s^{-1}$.

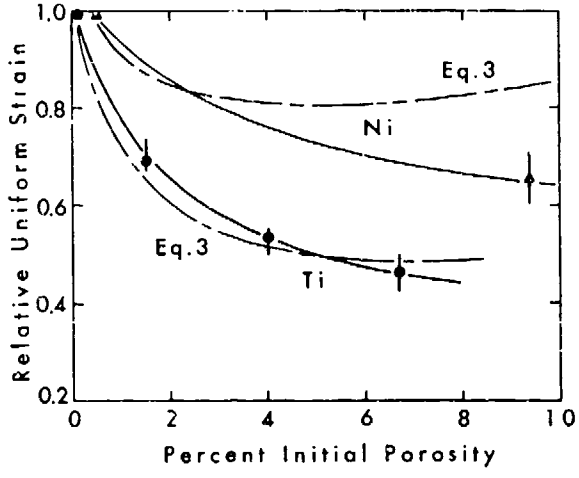


Figure 11. The dependence of uniform strain on initial porosity content for Ti and Ni as determined experimentally and as predicted from Eq. 3.